NUMERICAL INVESTIGATION ON THE ENERGETIC PERFORMANCES OF CONVENTIONAL AND PELLET AFTERTREATMENT SYSTEMS IN FLOW-THROUGH AND REVERSE-FLOW DESIGNS

Pietropaolo MORRONE, Angelo ALGIERI [*]

Mechanics Department, University of Calabria, Arcavacata di Rende (CS), Italy

The aim of the paper is the analysis of the energetic performances of structured and pelletized aftertreatment systems in flow-through and reverse-flow designs (passive and active flow control respectively) for diesel internal combustion engines. To this purpose, the influence of the engine operating conditions on the system performances has been investigated adopting a one-dimensional time-dependent model. Specifically, the thermal behaviour and the fuel saving capability of several arrangements have been characterized. The analysis has shown that the active emission control system with pelletized design guarantees higher heat retention capability. Furthermore, the numerical model has revealed the significant influence of the solid and exhaust gas temperature on the energy efficiency of the aftertreatment systems and the large effect of exhaust mass flow rate and unburned hydrocarbons concentration.

Key words: *Aftertreatment systems, internal combustion engines, energy efficiency, active flow control.*

1. Introduction

The technical evolution in the automotive industry has been mainly regulatory-driven. Specifically, within the last decades engine emissions have been reduced significantly adopting new aftertreatment strategies [1-5]. To this purpose, a host of investigations has been focused on oxidation catalysts (OCs), diesel particulate filters (DPFs), lean NO_x traps (LNTs), lean NO_x catalysts (LNCs) and selective catalytic reductions (SCRs) [6-12]. Nevertheless, further improvements are necessary to meet the more and more stringent exhaust regulations, to improve the energetic effectiveness of modern emission control systems and to balance costs and fuel economy benefits.

Nowadays, for the lean burn engine, energy efficient technologies to simultaneously remove particulate matters, CO, NO_x and HC are not available, and an integration of different systems is necessary [13-15]. Furthermore, the aftertreatment systems often require supplemental fuel to assure the proper thermal level for reliable processes and, as a consequence, a non-negligible fuel penalty and a deleterious impact on engine efficiency are produced [13,14]. As an example, high temperatures are required to regenerate diesel particulate filters, to initiate and to sustain light-off condition for oxidation catalysts and to permit the desulfurization process for lean NO_x traps [14,16].

[*] Corresponding author, e-mail: a.algieri@unical.it

Papadakis et al. put forward that there is an increasing trend in the NO_x reduction when the exhaust temperature for heavy-duty diesel engines raises [17]. Following Johnson [18], about 50-70% NO_x treatment on heavy-duty (HD) diesel engines will be needed at 500-520°C to meet the US NTE (Not-To-Exceed) regulations, established by the United States Environmental Protection Agency (US EPA).

In addition, selective catalytic reductions can demand high operating temperatures, depending both on the base oxides/metals used as active catalysts and on the reducing agents. Burch et al. showed, for instance, that alumina is very active for C_3H_6-SCR and selective to NO_x but only at high temperatures (i.e. above 400°C) [19].

Diesel Particulate Filters (DPFs) are very effective in reducing PM emissions. Specifically, DPF temperature should be raised at approximately 550-600°C in order to oxidize the trapped PM at a sufficient rate. As a consequence, a fuel penalty is associated with the regeneration process (also known as desoot) that ranges from 3 to 4.5%, depending on the desoot frequency regeneration [20,21]. Akmadza presented the fuel consumption - NO_x tradeoff curve for different engine technologies and he demonstrated that there is a 7% increase in the fuel penalty going from a Euro 5 calibration (0.18 g/km NO_x) to a Euro 6 calibration (0.080 g/km NO_x) [22]. Papadakis et al. highlighted that the fuel penalty in NO_x reduction experiments is also a function of the engine speed and torque, with a higher fuel consumption registered at idle condition [17].

At the same time, a fast heatup combustion strategy was proposed by Wada et al. for Lean NO_x Catalysts (LNCs) to keep the catalyst hot under cold or low load conditions but an instantaneous 6% fuel penalty was found to get the catalyst 43°C hotter [23].
Grumbrecht retrofited a Euro 4 sport utility vehicle with SCR behind the DPF to achieve Euro 6 NO_x levels. Preconditioning the catalyst with ammonia storage increased deNO_x efficiency by about 20% on the New European Drive Cycle (NEDC) test cycle, with a 4% increase in fuel consumption [24].

In order to reduce the fuel penalty, to increase the energy efficiency and to control the aftertreatment thermal level more efficiently, an innovative flow control (active control) has been developed in the last few years [14,25].

The active strategy is based on reversed flow converters and on the cyclic inversion of the exhaust gas between the two system ends (Figure 1). A cycle consists of forward and backward operations and it is defined as symmetric reverse flow if the two consecutive processes last the same time. Conversely, passive flow control represents the technical solution largely adopted in automotive practice with unidirectional flow within the emission control system.

The aim of the present work is the analysis and comparison of the energetic performances of active and passive aftertreatment systems with monolith and pelletized designs. The first system consists of structured monolith beds with several square cross-section thin channels. The second configuration employs randomly packed bed with spherical pellets (unstructured system).

A transient model has been proposed to assess the heat exchange between the solid and the exhaust gas, to calculate the energy effectiveness of the emission control systems and to evaluate the potential fuel saving capability of the active system with respect to the passive mode.
Specifically, the response of the system after sudden variations in engine load and the effect of the engine operating conditions on the energetic performances of emission control systems have been investigated.

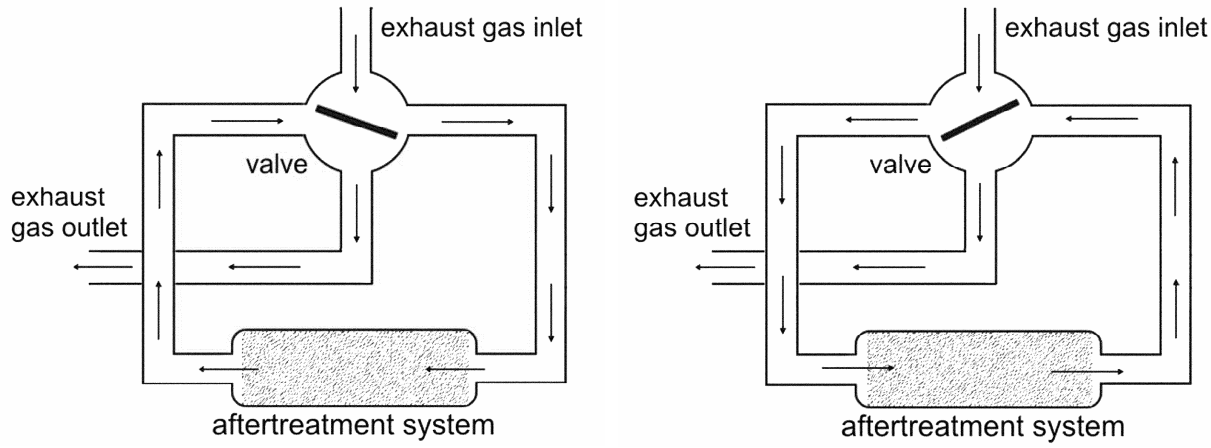

Figure 1 Active aftertreatment system: forward (a) and backward (b) operations.

2. Numerical Model

A one-dimensional transient model was developed to simulate the thermal exchange between the exhaust gas and the aftertreatment system. The main model assumptions are the following:

- working fluid as ideal mixture;
- constant mass flow rate;
- negligible thermal accumulation of the gas in the system;
- negligible conductive and radiative energy exchange mechanisms;
- adiabatic system towards the surroundings.

The composition of the exhaust gas was calculated from the combustion of $C_{12}H_{24}$ with excess air, in accordance with the literature [26]. An equivalent mass flow rate of methane, that is representative of the combined exhaust HC and CO in average Diesel, has been assumed in order to calculate the oxidation of the unburned hydrocarbons HC that are present in the exhaust gas [14].

The catalytic reactions are not taken into account and the results can be extended to a generic automotive aftertreatment system. Although the behaviour of the aftertreatment systems depends also on different practical aspects, such as pulsating flow, engine vibration, road shock and proper location of the converter, the evaluation of their influence goes beyond the scope of this paper.

The model was applied to two emission control configurations with ceramic substrate: monolith structured and pellet unstructured design.

2.1 *Monolith Structured Design*

The structured monolith usually consists of blocks having longitudinal square holes with about 1 mm x 1 mm channel flow area [13]. The thermal exchange can be described as follows:

$$\frac{\partial T}{\partial x} = \frac{h \cdot (P / A_c) \cdot (T_s - T)}{G \cdot c_p} \tag{1}$$

$$\rho_s \cdot c \cdot S \cdot dx \cdot \frac{\partial T_s}{\partial t} = \dot{q}_{ex} \cdot P \cdot dx - G \cdot A_c \cdot c_p \cdot dT \tag{2}$$

where h is the heat transfer coefficient;

x is the longitudinal coordinate;

P is the channel perimeter;
A_c is the cross area of a single channel;
T is the gas temperature;
T_s is the solid temperature;
G is the mass flow rate per unit area A_c;
c_p is the specific heat of the working fluid;
c is the specific heat of the solid phase;
ρ_s is the solid density;
S is the area of solid cross-section;
t is the generic time;
$\dot{q}_{ex}$ is the exothermic energy generation rate per unit area, related to the oxidation of the equivalent methane.

The ratio (P/A_c) is the exchange surface per unit volume of the bed and $S\,dx$ is the volume of solid that exchanges thermal energy with the gas.

A thermal calculation was adopted in the model and the energetic contribution of oxidation was equally distributed over the whole channel according to Zheng and Reader [14]. As a consequence, the exothermic reaction of the fluid was treated as surface heat generation and no assumptions of light-off temperature for the catalyst were assumed:

$$\dot{q}_{ex} = \frac{\dot{m}_{CH_{4Eq}} \cdot LHV}{P \cdot L} \tag{3}$$

where LHV is the lower heating value;
L is the monolith length;
$\dot{m}_{CH_{4Eq}}$ is the equivalent methane mass flow rate.

For the complete resolution of the problem, the further following equations were considered:

$$\frac{\partial (\rho u)}{\partial x} = 0 \tag{4}$$

$$\frac{\partial p}{\partial x} = -\frac{1}{2 \cdot D_{eq}} \cdot f \cdot \rho \cdot u^2 \tag{5}$$

$$p = \rho \cdot R^* \cdot T \tag{6}$$

where u is the gas velocity;
ρ is the gas density;
p is the gas pressure;
D_{eq} is the channel hydraulic diameter.

The momentum balance equation for a fixed bed is taken into account through the equation 5 that depends on the Fanning coefficient f, equal to 64/Re for laminar flow, as occurs in the operative conditions of this paper.

As far as the heat transfer coefficient is concerned, various correlations are present in the literature. Specifically, there are correlations for laminar or turbulent flow, for constant heat flux or constant solid temperature [27,28]. The heat transfer coefficient h was obtained as a function of Reynolds (Re) and Prandtl (Pr) numbers, using the correlation attributed to Hausen [29] and adopted by Rafidi and Blasiak [30] to study the thermal exchange within a structured monolith:

$$Nu = h \cdot \frac{D_{eq}}{k} = 3.61 + \frac{0.0668 \cdot (D_{eq} / L)\, Re\, Pr}{1 + 0.04 \cdot \left[(D_{eq} / L)\, Re\, Pr\right]^{2/3}} \tag{7}$$

The equations were solved with a finite difference scheme. More detail on the model is reported in the literature [31,32].

2.2 *Pellet Unstructured Design*

The unstructured converter consists of a bed of spherical pellets with typically 3 mm diameter [13]. The thermal exchange in the packed bed with forced fluid flow was described through the following equations:

$$\frac{\partial T}{\partial x} = \frac{h \cdot a \cdot (T_s - T)}{G \cdot c_p} \tag{8}$$

$$\rho_s\ c\ A\ dx(1-\varepsilon) \cdot \frac{\partial T_s}{\partial t} = \dot{q}_{ex}\ a\ A\ dx - G\ A\ c_p dT \tag{9}$$

where a is the wetted surface of the packed bed per unit volume;

ε is the porosity, assumed to be uniform within the bed;

A is the cross section of the pellet bed system.

The energetic contribution of oxidation was evaluated as following:

$$\dot{q}_{ex} = \frac{\dot{m}_{CH_{4Eq}} \cdot LHV}{a \cdot A \cdot L} \tag{10}$$

while the wetted surface of the packed bed per unit volume was expressed by:

$$a = \frac{6(1-\varepsilon)}{\varphi_s d_s} \tag{11}$$

where d_s is the pellet diameter and φ_s is the sphericity of particles, which is the ratio of the sphere surface to the real surface of the particle. Therefore, sphericity is equal to 1 only for spherical particles, while it is lower for packing units of different shape.

The hypothesis of negligible temperature gradients within particles was assumed because the Biot number $Bi = h\,(d_s / 6\varphi_s) / k_s$ was lower than 0.1 [33].

Pressure losses were evaluated by the semi-empiric Ergun equation [27], which relates pressure to superficial velocity in a porous medium:

$$\frac{\partial p}{\partial x} = -\frac{150 \cdot (1-\varepsilon)^2 \cdot \mu}{\varphi_s^2 \cdot d_s^2 \cdot \varepsilon^3} \cdot u - \frac{1.75 \cdot (1-\varepsilon)}{\varphi_s \cdot d_s \cdot \varepsilon^3} \cdot \rho \cdot u^2 \tag{12}$$

Various correlations are present in literature for the heat transfer coefficient and yield very different values [34-37]. In the present work, the well-established and rather conservative relation proposed by Kunii e Levenspiel [36] was adopted:

$$Nu = \frac{h \cdot d_s}{k} = 2 + 1.8 \cdot Pr^{\frac{1}{3}} \cdot Re^{\frac{1}{2}} \tag{13}$$

with $Re > 100$.

The model was validated with experimental results with a good agreement with respect to the experimental data. The average error for the gas temperature data was 2%, while for the bed temperature was lower than 6% [38].

3. Operative conditions and performance parameters

The geometric characteristics and the operating conditions of the monolith and pelletized aftertreatment system are shown in Table 1 for a diesel engine with 6-dm^3 displacement and 150 kW power.

To analyse the energy performance of the emission control system, the "*aftertreatment cooling process"* was examined. Particularly, the initial solid temperature was set at 700°C, while the exhaust gas temperature was fixed at 200°C. This corresponds to a sudden decrease in the engine load after long full load operation [14].

Therefore, at the beginning of the cooling process, the emission control system presents a maximum internal energy value:

$$E_{max} = m \cdot c \cdot T_{s,0} \tag{14}$$

where m is the solid mass;

$T_{s,0}$ is the initial temperature of the solid.

For simplicity, the internal energy is assumed zero when the temperature is equal to 0 K.

The low temperature gas flow determines the progressive cooling of the solid. Specifically, the minimum energy state corresponds to the complete cooling of the aftertreatment system:

$$E_{min} = m \cdot c \cdot T_{inlet} \tag{15}$$

where T_{inlet} is the exhaust gas temperature.

The heating process was not considered in the following analysis. In fact, previous works showed that the active control system is not recommended during the warm-up phase, if a rapid heating process is required [39,40].

Table 1 Operative conditions for the working fluid and emission control systems.

Reference converter size, H W L *(height; width; length)*	141 141 300 mm mm mm
Exhaust flow rate, $\dot{m}$	50 - 200 g/s
Methane mass flow rate, $\dot{m}_{CH_{4\,Eq}}$	0.00 - 0.30 g/s
Exhaust gas temperature, T_{inlet}	200 - 600°C
Initial solid temperature, T_s	400 - 700°C
Solid phase density, ρ_s	2807 kg/m^3
Solid specific heat capacity, c	800 J/kg K
Monolith Design	
Cell density, c_d	62 cell/cm^2
Channel size, b	0.90 mm
Wall thickness, w	0.35 mm
Monolith mass, m	8.40 kg
Wetted surface per unit volume, S_w/V	2201 m^{-1}
Pellet Design	
Spheres diameter, d_s	3 mm
Porosity, ε	44%
Pellet packed bed mass, m	9.37 kg
Wetted surface per unit volume, a	1120 m^{-1}

3.1 *Stored Energy Fraction (SEF)*

The evaluation of the aftertreatment energetic performance was achieved through a dimensionless parameter, the Stored Energy Fraction (SEF) [39-41]:

$$SEF = \frac{E(t) - E_{min}}{E_{max} - E_{min}} \tag{16}$$

where $E(t)$ is the thermal energy stored in the solid at time t:

$$E(t) = \frac{m \cdot c \cdot \int_0^L T_s(x,t) \cdot dx}{L} \tag{17}$$

The fraction of the stored thermal energy is a function of time and thus represents a heat retention efficiency. The *SEF* parameter permits to compare the thermal characteristics of different aftertreatment systems (active and passive flow control, structured and unstructured design), independently of the operating conditions (i.e. exhaust gas temperature, initial solid temperature) and to evaluate the system response to fast variations in the engine load.

3.2 *Dimensionless Saved Fuel (DSF)*

The energy saving capability of the active systems with respect to the passive control has been also expressed in terms of a potential Dimensionless Saved Fuel (*DSF*). It represents the ratio between the fuel that could be saved adopting the active system and the corresponding engine fuel consumption and it is defined as follows [42]:

$$DSF = \frac{\int_0^t \dot{m}_{saved\ fuel}\, dt}{\dot{m}_{fuel}\, t} \tag{18}$$

where $\dot{m}_{saved\ fuel}$ is the supplemental fuel that should be added to the passive aftertreatment system to guarantee the same mean temperature of the active apparatus, $\dot{m}_{fuel}$ represents the corresponding fuel that is burned within the combustion chamber and t is the generic operating time.

4. Results

The proposed transient model was adopted to analyze the energetic performances of emission control systems with active and passive flow control. Furthermore, monolith and pellet designs were considered. For the reversed flow control mode, a symmetrical thermal cycle was investigated.

Figure 2 highlights the temperature profiles of solid phase along the monolith and the pellet packed bed as a function of time for the passive flow control mode.

The exhaust gas temperature is set equal to 200°C while the initial solid temperature is 700°C. This operating condition simulates the exhaust gas at low engine load after a long period of high load operation [14]. The analysis put in evidence the significant influence of time on the temperature distribution within the emission control system. The pellet packed bed system guarantees higher temperature values than the monolith one. However, the temperature differences between the two designs tend to reduce with the operating time and become negligible after 100 seconds. At this time,

an increase by nearly 66°C is registered in the rear part of both systems, due to the contribution of unburned hydrocarbons oxidation. As far as the gas temperature is concerned, a similar behavior is observed. To this purpose, previous works showed that temperature differences between the solid and gas phase are low and reduce with the operating time [39,40].

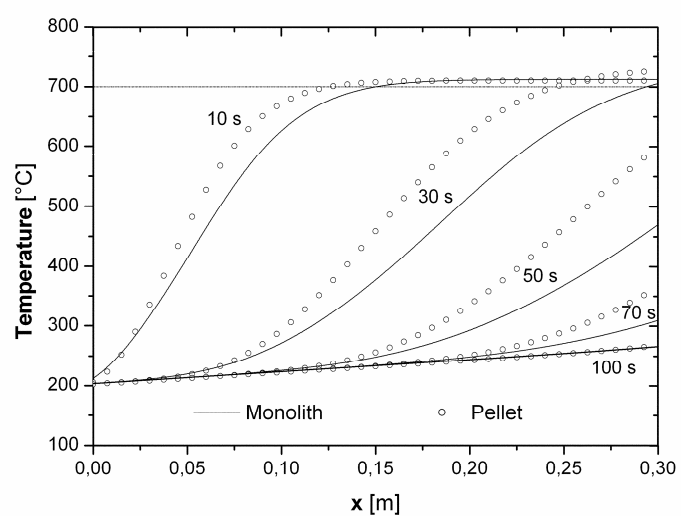

Figure 2 Temperature profiles of the solid phase along the aftertreatment system as a function of time for monolith and pellet arrangements. Passive flow control.

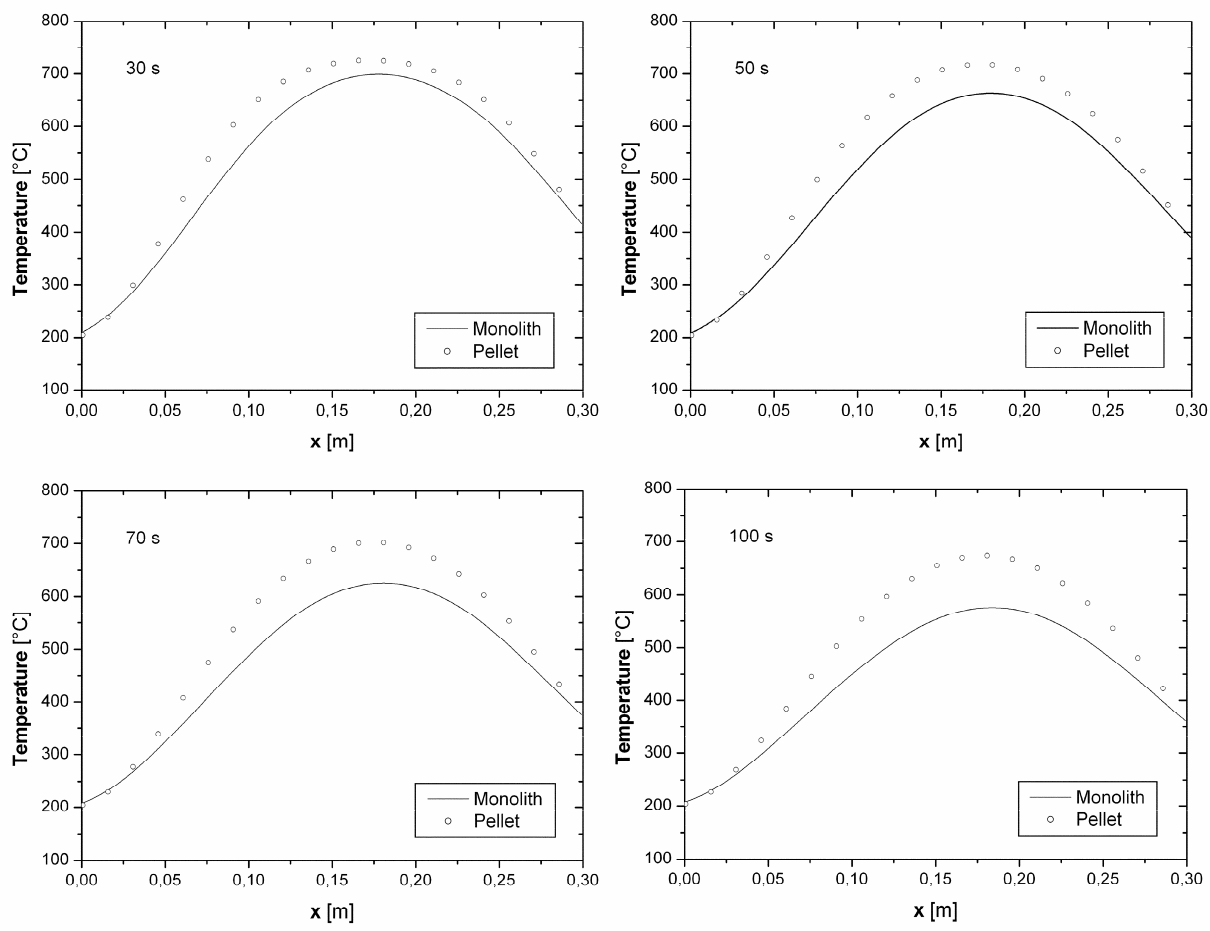

Figure 3 Temperature profiles of the solid phase along the aftertreatment system as a function of time for monolith and pellet arrangements. Active flow control.

A different temperature distribution within the emission control system is found when the reverse flow operation is adopted. The evolution of solid temperature profiles in a range of 100 seconds is illustrated in Figure 3. A maximum temperature value is located at the central region of the device, with a progressive decrease with the operating time. Specifically, for the structured design the maximum temperature moves from about 700°C at 30 seconds to 575°C at 100 seconds. For the unstructured system the corresponding decrease is from about 725°C at 30 seconds to 675°C at 100 seconds.

The comparison between the different designs shows that the pellet packed configuration presents a larger retention capability for the considered channel and sphere sizes (Table 1). Furthermore, the active flow control guarantees the greater energetic performance. Particularly, for passive control systems, the solid phase is almost completely cooled after 100s, except for the oxidation contribute. On the other hand, the reverse flow control assures significantly higher temperature values in the central area of the system, with an increase of about 340°C and 440°C for the monolith and pelletized design respectively. Therefore, the active technique permits a significant energy saving with respect to the passive control strategy, even under lean mixture conditions and low load operation, without additional fuel. Figure 4a, in fact, presents the comparison between the stored energy fractions for both the control modes and the two configurations. The analysis put in evidence that the dimensionless stored energy fraction (SEF) parameter is independent of the system configuration when the passive control is adopted. Specifically, the thermal retention effectiveness of the two passive systems falls to about 7% after 90 s. The corresponding values for the active flow control are about 53% and 65% with the monolith and pellet converters respectively. In these cases, SEF values become about 29% and 45% after 300 seconds.

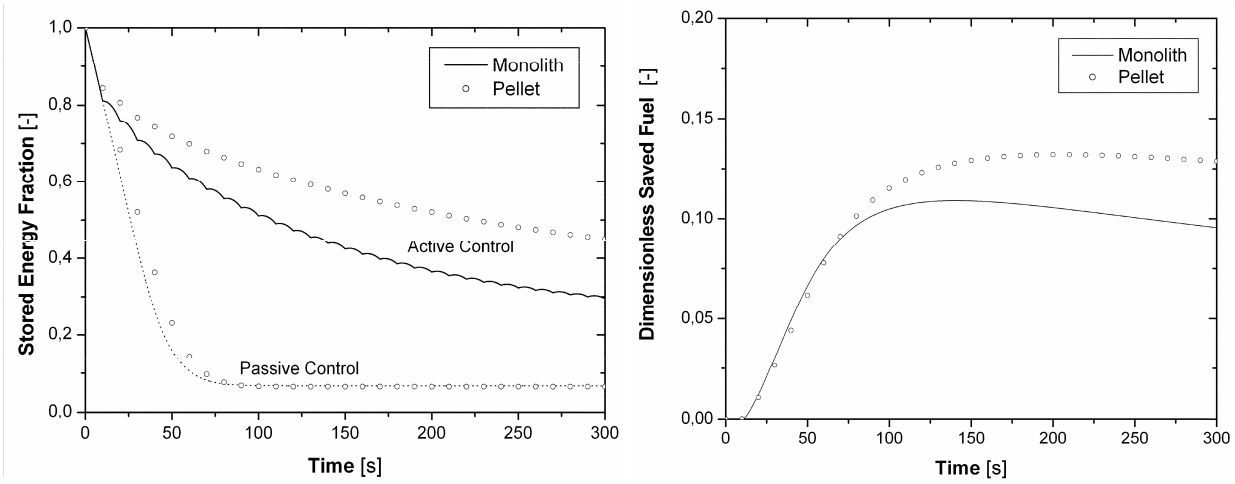

a) b)

Figure 4 Stored energy fraction with active and passive flow control (a) and dimensionless saved fuel (b) as a function of time for monolith and pellet configurations.

The energy saving capability of the reversal operation, with respect to the unidirectional flow control, has been also evaluated considering the potential dimensionless saved fuel (DSF).

Figure 4b depicts that the difference between monolith and pellet arrangements is negligible until 70s and tends to upsurge with the operating time. The better performances are registered using the pelletized emission control apparatus. After 5 minutes the DSF tends to a percentage value of 9.5 and 12.9 for structured and pellet configuration respectively.

Pressure drops for pellet and monolith emission control systems are visible in Figure 5. The analysis reveals that the reverse control causes higher values, especially for the pellet design. The consequence is a higher negative influence on the engine performances, that could be improved by a proper choice of the pellet size. Pressure loss reduce with time due to the progressive temperature decrease. The maximum value is lower than 6 kPa for the monolith systems while the pelletized configurations present pressure drops larger than 24 kPa. Furthermore, a slight additional backpressure is related to the periodic flow inversion (200 - 500 Pa), with the larger value registered for the pellet packed bed.

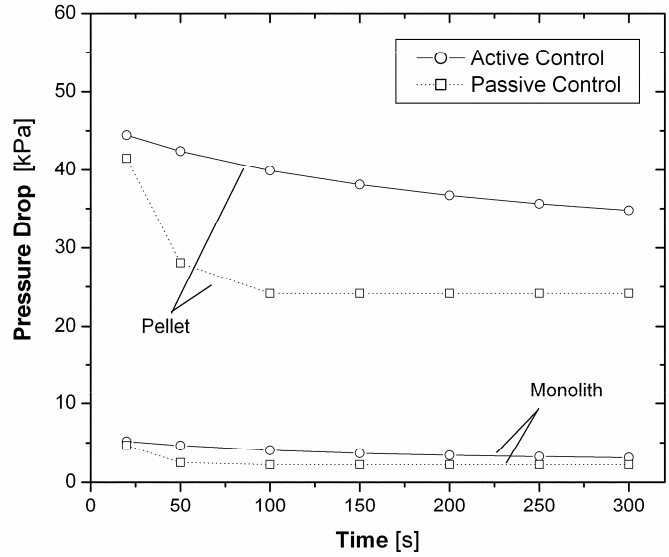

Figure 5 Pressure drops as a function of time for monolith and pellet packed bed.

4.1 *Effect of solid and exhaust gas temperature*

The previous analysis demonstrates that structured emission control system guarantees lower pressure drops with respect pelletized system, while the unstructured design presents a significant higher thermal retention and saved fuel capability.

In order to study the effect of the engine load on the energetic performance of the emission control systems, the influence of the exhaust gas and solid temperature were investigated. Figure 6 highlights the stored thermal energy fraction for three exhaust gas temperature values (200, 400 and 600°C) while the initial temperature of the aftertreatment is 700°C .

A previous work revealed that the dimensionless SEF parameter is roughly independent of the exhaust gas temperature if the unburned hydrocarbons oxidation is absent [39]. Conversely, Figure 6 reveals that the chemical reactions determine important differences in the stored energy fraction values for the different exhaust temperatures. As expected, the higher the exhaust gas temperature, the higher the SEF value. For the passive control the dimensionless parameter presents the same values for monolith and pellet aftertreatment system configuration (Figure 6a), while there are significant differences for the active mode. Specifically, the higher SEFs are found for the pelletized system. Furthermore, Figure 6b depicts that the stored energy fraction is larger than 100% when the active control is adopted and the exhaust gas temperature is 600°C. In fact, the higher efficiency of the reverse flow operation, the chemical reactions in the exhaust unburned gas and their high initial

thermal level produce temperatures higher than the initial solid temperature. In these cases, attention should be focused on the temperature distribution within the aftertreatment apparatus due to the system potential overheat and/or to the serious aging and durability problems that could appear when high temperatures are reached.

The exhaust gas temperature has also a significant influence on the fuel mass that could be saved adopting the active system. Figure 7 refers to the previous three exhaust gas temperatures (200, 400 and 600°C) with the same initial solid thermal level (700°C). If the exhaust gas temperature raises the difference between the mean temperature of active and passive flow control decreases. As a consequence, the higher the exhaust gas temperature, the lower the saved fuel. As an example, after 300 seconds the dimensionless saved fuel mass values of the monolith aftertreatment system are 5.1, 7.6 and 9.5% for 600, 400 and 200°C respectively. The corresponding values of the unstructured design are 5.6, 9.4 and 12.9%.

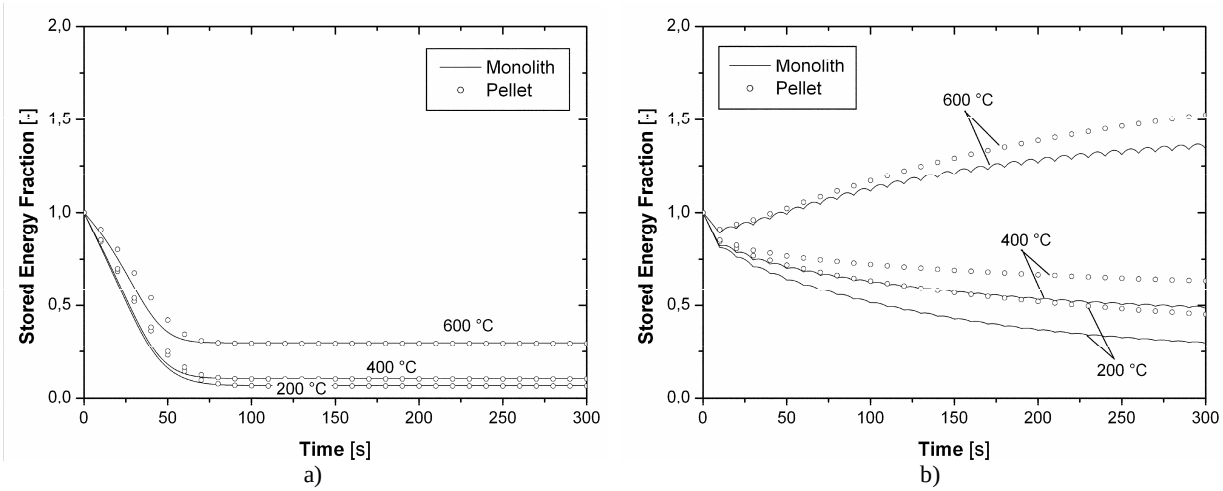

Figure 6 Influence of the exhaust temperature on the stored energy fraction with passive (a) and active (b) flow control for monolith structured and pellet unstructured bed configuration.

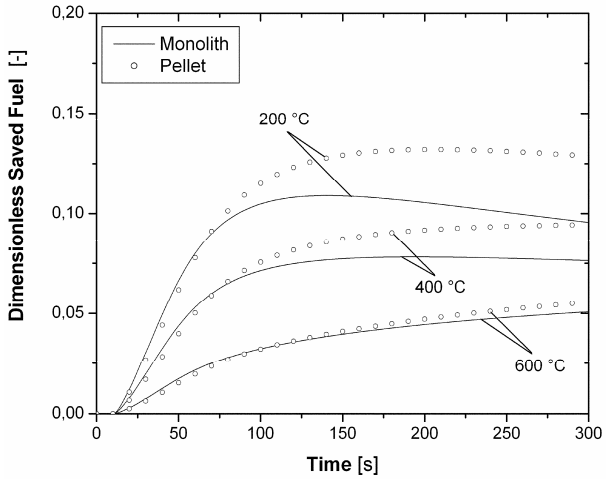

Figure 7 Influence of exhaust temperature on dimensionless saved fuel for monolith and pellet systems.

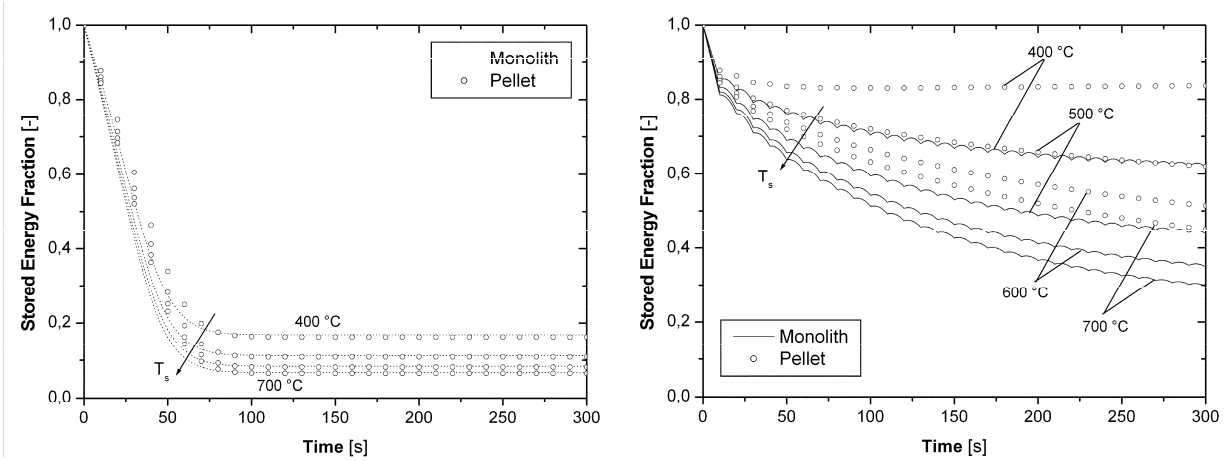

a) b)

Figure 8 Influence of the solid temperature on the stored energy fraction with passive (a) and active (b) flow control for monolith structured and pellet unstructured bed configuration.

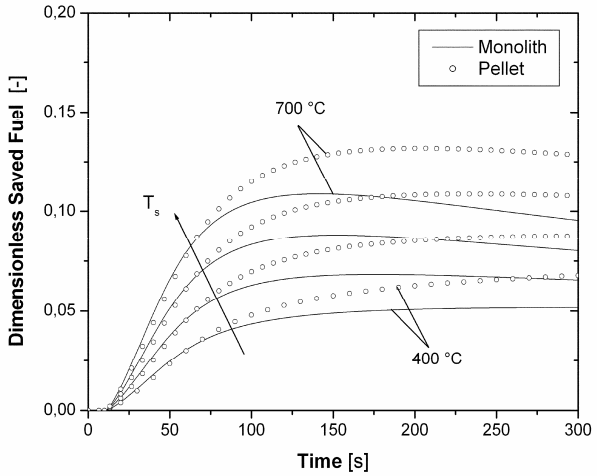

Figure 9 Influence of the solid temperature on the dimensionless saved fuel.

Moreover, the influence of the solid temperature on the performances of emission control systems was evaluated. To this purpose four initial solid temperatures were considered (400, 500, 600 and 700°C) with the same feed gas temperature (200°C). The analysis put forward the large influence of the initial solid thermal level on the energetic characteristics of the systems. Specifically, the lower the solid temperature, the higher the heat retention capability (Figure 8) and the lower the dimensionless saved fuel (Figure 9). Particularly, when the temperature of the device goes from 400 to 700°C, the dimensionless saving fuel capability moves from 5.2 to 9.5% for the monolith arrangement after 300 seconds. The corresponding DSF value for the pelletized configuration changes from 6.8 to 12.9%.

4.2 *Effect of exhaust gas and unburned hydrocarbons mass flow rate*

Figures 10 and 11 show the influence of the exhaust gas flow rate on SEF and DSF parameters considering the same percentage amount of unburned hydrocarbons in the exhaust gas (0.15%). The decrease in stored energy fraction with operating time is significantly lower for the active system, due to its better thermal retention. Furthermore, Figure 10a reveals that the asymptotic

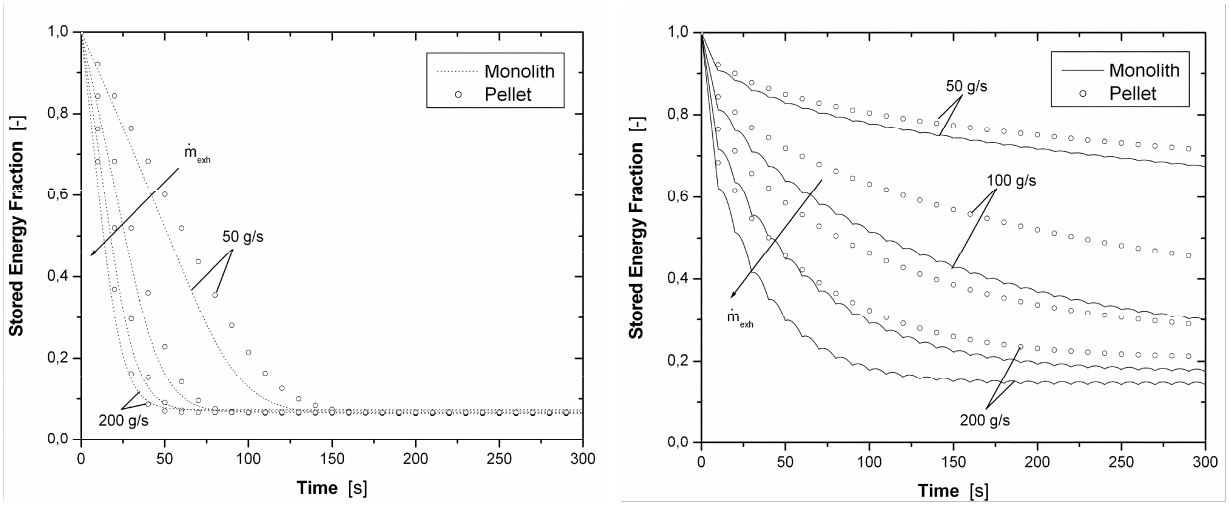

Figure 10 Influence of the exhaust mass flow rate on the stored energy fraction with passive (a) and active (b) flow control for monolith structured and pellet unstructured bed configuration.

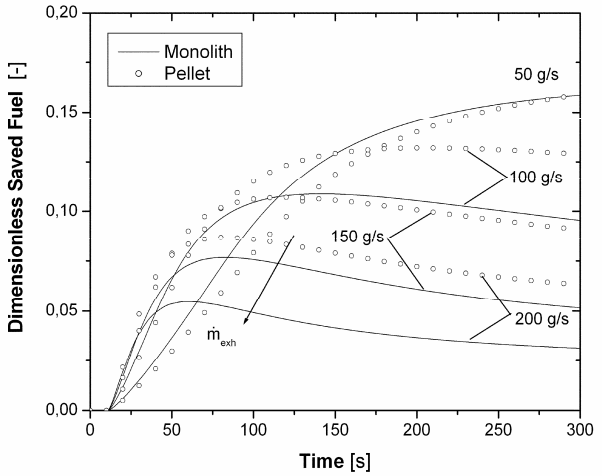

Figure 11 Influence of the exhaust mass flow rate on the dimensionless saved fuel.

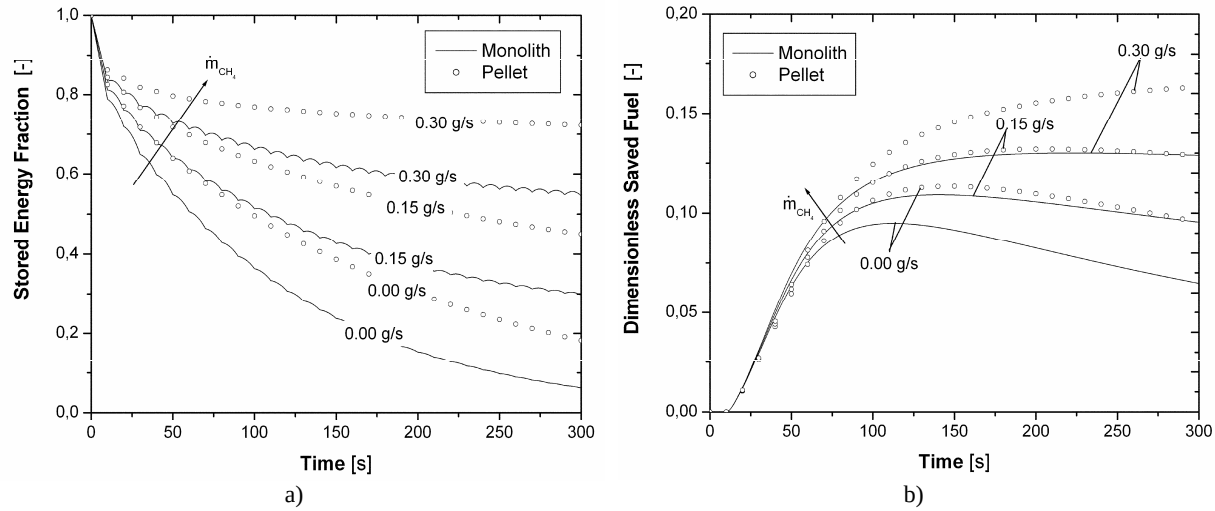

Figure 12 Influence of HC concentration on the stored energy fraction with active flow control (a) and dimensionless saved fuel (b) for monolith structured and pellet unstructured bed configuration.

values for the passive system are almost the same for all the investigated exhaust mass flow rates (about 6.5%), whereas for the active flow control the lower the exhaust mass flow rates, the higher the SEF values. After 300 s, for the reversal operation, the stored energy fraction of the monolith arrangement decreases from about 0.67 to 0.14 when the exhaust flow rate passes from 50 to 200 g/s. The corresponding SEF values for the unstructured design are 0.71 and 0.21 . The outlined difference between the two flow control modes is also evident in terms of dimensionless saved fuel, that upsurges with the decrease in the exhaust mass flow rate.

Finally, the influence of the unburned hydrocarbons mass flow rate in the exhaust gas was investigated. Specifically, three equivalent methane concentrations were used (0.00, 0.15 and 0.30 g/s), considering the same exhaust mass flow rate (100 g/s). The analysis in terms of the stored energy fraction was focused on the active reverse flow control, due to its greater efficiency. An increasing trend of SEF values is registered with the unburned concentrations (Figure 12a) due to the increasing oxidation effect. A plateau is reached when the convective heat transfer effect becomes negligible and it is proportional to the equivalent methane content. The pellet packed configuration guarantees higher stored energy fraction values. However, when no oxidation occurs the SEF values tend to zero for both monolith and pellet packed bed.

The higher retention capability of the pelletized aftertreatment system produces also a larger saving fuel capability (Figure 12b). As an example, the values of the dimensionless saved fuel with monolith arrangement and 0.30 g/s of unburned hydrocarbons correspond to the values obtained with 0.15 g/s HC and pellet packed bed.

Furthermore, the plot shows that the larger the HC content, the larger the dimensionless saved fuel mass. In particular, after 5 minutes DSF for monolith moves from 6.5 to 12.9% passing from 0.00 g/s (no HC oxidation) to 0.30 g/s of equivalent methane. The corresponding values for the pelletized aftertreatment system are 9.6 and 16.3% respectively.

5. Conclusions

A transient model was developed to analyze the energetic performances of active and passive aftertreatment systems with monolith and random packed bed configurations and to evaluate the influence of the engine operating conditions on the process characteristics. In particular, two dimensionless parameters were defined as a function of the temperature profiles: the stored energy fraction and the potential dimensionless saved fuel.

The comparison between the different flow control modes showed the greatest thermal inertia of the flow inversion operation. In fact, the active flow control is more appropriate to maintain the initial temperature level of the emission control system for a longer time after sudden variations in engine load. This is true even under lean mixture conditions and low load operations, without the addition of supplemental fuel. Thus, the active technique allows significant fuel savings with respect to the passive strategy.

Furthermore, the comparison between different system configurations gave evidence that the active pellet emission control system guarantees a significantly higher thermal retention and saved fuel capability with respect to the structured design. On the other hand, the pelletized system presents larger pressure drops and produces a negative influence on the engine performances. The proper

choice of the pellet size becomes crucial to reduce this effect and therefore future works will be addressed to the evaluation of this issue.

In addition, the simulations revealed the significant influence of the exhaust gas and solid temperatures on the stored energy fraction and dimensionless saved fuel, with a larger effect that was found for the active flow control. For both geometric configurations, SEF values increase with the exhaust temperature and decrease with the solid temperature. An opposite trend was observed for the DSF parameter. Finally, the study evidenced the great impact of the exhaust mass flow rate and unburned hydrocarbons concentration on the aftertreatment systems performance. Particularly, the better results were registered with the lower exhaust flow rate and the higher HC content due to the increasing oxidation effect.

Nomenclature

A	Aftertreatment cross area [m^2];	$\dot{m}_{CH_{4\,Eq}}$	Methane mass flow rate [kg/s];
a	Packed bed wetted surface [m^{-1}];	$\dot{m}_{fuel}$	Burned fuel [kg/s];
A_c	Channel cross area [m^2];	$\dot{m}_{saved\,fuel}$	Potential saved fuel [kg/s];
b	Channel dimension [m];	NEDC	New European Drive Cycle;
Bi	Biot number [-];	NO_x	Nitrogen oxides;
CO	Carbon monoxide;	NTE	Not to exceed;
c	Specific heat of the solid phase [J/kg K];	Nu	Nusselt number [-];
c_d	Cell density [cell/cm^2];	OC	Oxidation catalyst;
c_p	Specific heat of the gas [J/kg K];	P	Channel perimeter [m];
D_{eq}	Channel hydraulic diameter [m];	p	Gas pressure [Pa];
d_s	Sphere diameter [m],	PM	Particulate matter;
DPF	Diesel particulate filter;	Pr	Prandtl number [-];
DSF	Dimensionless Saved Fuel [-];	ρ	Gas density [kg/m^3];
$E(t)$	Thermal energy at time t [J];	ρ_s	Solid density [kg/m^3];
EPA	Environmental Protection Agency;	$\dot{q}_{ex}$	Exothermic energy generation [W/m^2];
ε	Porosity or void fraction [-];	R^*	Specific gas constant [J/kg K];
f	Fanning friction coefficient [-];	Re	Reynolds number [-];
φ_s	Particle sphericity [-];	S	Area of solid cross-section [m^2];
G	Mass flow rate per unit area [kg/s m^2];	SCR	Selective catalytic reduction;
H	Converter height [m];	SEF	Stored Energy Fraction [-];
h	Heat transfer coefficient [W/m^2 K];	S_w/V	Wetted surface per unit volume [m^{-1}];
HC	Hydrocarbons;	t	Time [s];
k	Thermal conductivity [W/m K]	T	Gas temperature [°C];
LHV	Lower heating value [J/kg];	T_s	Solid temperature [°C];
L	Converter length [m];	T_{inlet}	Inlet gas temperature [°C];
λ	Relative air/fuel ratio [-];	TWC	Three-way catalyst;
LNC	Lean NO_x catalyst;	u	Gas velocity [m/s];
LNT	Lean NO_x trap;	x	Longitudinal coordinate [m];
m	Solid mass [kg];	W	Converter width [m];
$\dot{m}$	Exhaust flow rate [kg/s]	w	Channel thickness [m].

References

[1] Tan, P. Q., Hu, Z. Y., Deng, K. Y., Lu, J. X., Lou, D.M., Wan, G., Particulate matter emission modelling based on soot and SOF from direct injection diesel engines, *Energy Conversion and Management, 48* (2007), 2, pp. 510-518.

[2] Johnson, T. V., Diesel Emission Control in Review, *SAE International Journal of Fuels and Lubricants, 2* (2009), pp. 1-12.

[3] Kesgin, U., Study on prediction of the effects of design and operating parameters on NO_x emissions from a leanburn natural gas engine, *Energy Conversion and Management, 44* (2003), 6, pp. 907-921.

[4] Iwamoto, J., Wada, K., Shiraishi, R., Mikami, H., Motohashi, G., Ohno, H., Feasibility Study of NOx Reduction with the Active Exhaust Control System when Engine Starting, *Proceedings*, FISITA 2010 World Automotive Congress, Budapest, Hungary, 2010.

[5] Petrović, V. S., Particulate Matters from Diesel Engine Exhaust Emission, *Thermal Science, 12* (2008), 2, pp. 183-198.

[6] Pontikakis, G., Stamatelos, A., Three-Dimensional Catalytic Regeneration Modeling of SiC Diesel Particulate Filters, *Journal of Engineering for Gas Turbines and Power, 128* (2006); pp. 421-433.

[7] Filipi, Z., Hagena, J., Fathy, H., Investigating the impact of in-vehicle transients on diesel soot emissions, *Thermal Science, 12* (2008), 1, pp. 53-72.

[8] Petković, S. D., Pešić, R. B., Lukić, J. K., Heat transfer in exhaust system of a cold start engine at low environmental temperature, *Thermal Science, 14* (2010), Suppl., pp. S209-S220.

[9] Lehtoranta, K., Matilainen, P., Kinnunen, T.-J. J., Heikkilä, J., Rönkkö, T., Keskinen, J., Murtonen, T., Diesel Particle Emission Reduction by a Particle Oxidation Catalyst *Proceedings*, SAE 2009 Powertrains Fuels and Lubricants Meeting, San Antonio, USA, SAE paper 2009-01-2705, 2009.

[10] Kim, D. S., Park, Y. J., Lee, S. W., Cho, Y. S., A study on characteristics and control strategies of cold start operation for improvement of harmful exhaust emissions in SI engines, *Journal of Mechanical Science and Technology, 22* (2008), pp. 141-147.

[11] Ji, Y., Fisk, C., Easterling, V., Graham, U., Poole, A., Crocker, M., Choi, J.-S., Partridge, W., Wilson, K., NO_x storage–reduction characteristics of Ba-based lean NO_x trap catalysts subjected to simulated road aging, *Catalysis Today, 151* (2010), 3-4, pp. 362-375.

[12] Kowatari, T., Hamada, Y., Amou, K., Hamada, I., Funabashi, H., Takakura, T., Nakagome, K., A Study of a New Aftertreatment System (1): A New Dosing Device for Enhancing Low Temperature Performance of Urea-SCR, *SAE Transactions - Journal of Fuels and Lubricants, 115* (2006), pp. 244-251.

[13] Heywood, J. B., Internal Combustion Engine Fundamentals, Mc Graw Hill, New York, 1988.

[14] Zheng, M., Reader, G. T., Energy efficiency analyses of active flow aftertreatment systems for lean burn internal combustion engines, *Energy Conversion and Management, 45* (2004), pp. 2473-2493.

[15] Güthenkea, A., Chatterjeea, D., Weibela, M., Waldbüßera, N., Kočíb, P., Marekb, M., Kubíčekc, M., Development and application of a model for a NOx storage and reduction catalyst, *Chemical Engineering Science, 62* (2007), pp. 5357-5363.

[16] Cauda, E., Fino, D., Saracco, G., Specchia, V., Preparation and regeneration of a catalytic diesel particulate filter, *Chemical Engineering Science, 62* (2007), pp. 5182-5185.

[17] Papadakis, K., Odenbrand, C. U. I., Creaser, D., Stationary NOx Storage and Reduction Experiments on a Heavy-Duty Diesel Engine Rig Using a Bypass System, 2003, SAE Paper 2003-01-1884.

[18] Johnson, T. V., Diesel Emission Control in Review, *SAE Transactions - Journal of Fuels and Lubricants, 115* (2006), pp. 1-15.

[19] Burch, R., Breen, J. P., Meunier, F. C., A review of the selective reduction of NOx with hydrocarbons under lean-burn conditions with non-zeolitic oxide and platinum group metal catalyst, *Applied Catalysis B: Environmental, 39* (2002), pp. 283-303.

[20] Adelman, B., Karkkainen, A., Berke, P., Heibel, A., Parker, T., Pickles, D., Development and Application of a US-EPA ´07 Particulate Filter System for a 7.6l I-6 Medium Duty Truck Engine, *Proceedings*, 15th Aachen Kolloquium Fahrzeug- und Motorentechnik, Aachen, Germany, 2006.

[21] Parks II, E., Prikhodko, V., Storey, J. M. E., Barone, T. L., Lewis, Sr. S. A., Kass, M. D., Huff, P., Emissions from premixed charge compression ignition (PCCI) combustion and affect on emission control devices, *Catalysis Today, 151* (2010), pp. 278–284.

[22] Akmadza, F., Status of the Euro 5/6 Legislation and Impact on Passenger Cars Engine Development and After Treatment Technology, *Proceedings*, Car Training Institute DPF Forum, Frankfurt, Germany,2007.

[23] Wada, K., Suzuki, N., Satoh, N., Morita, T., Yamaguchi, S., Ohno, H., Study on Emission Reducing Method with New Lean NOX Catalyst for Diesel Engines, 2007; SAE paper 2007-01-1933.

[24] Grumbrecht, F., Krämer, L., Mönnig, R., Op de Beeck, J., Hünnekes, E., Joubert, E., Concept Development of an SCR Demonstrator Vehicle, *Proceedings*, Meeting Future European Emission Limits with Low Fuel Consumption. IAV MinNOx Conference, Berlin, Germany, 2007.

[25] Liu, B., Hayes, R. E., Checkel, M. D., Zheng, M., Mirosh, E., Reversing flow catalytic converter for a natural gas/diesel dual fuel engine, *Chemical Engineering Science, 56* (2001), pp. 2641-2658.

[26] Singh, P., Thalagavara, A. M., Naber, J. D., Raux, S., Dorge, S., Gilot, P., Climaud, P., Sassi, A., Johnson, J., Bagley, S., An Experimental Study of Active Regeneration of an Advanced Catalyzed Particulate Filter by Diesel Fuel Injection Upstream of an Oxidation Catalyst. *SAE Transactions - Journal of Fuels and Lubricants, 115* (2006) pp. 334-357.

[27] Perry, R. H., Green, D. W., Perry's chemical engineers' handbook, 7th edition. Mc Graw Hill, New York, 1999.

[28] Guglielmini, G., Pisoni, C., Elementi di trasmissione del calore, Veschi Edizioni, Milano, 1990.

[29] Incropera, F., De Witt, D., Fundamentals of Heat and Mass Transfer, Wiley & Sons, USA, 2002.

[30] Rafidi, N., Blasiak, W., Thermal performance analysis on a two composite material honeycomb heat regenerators used for HiTAC burners, *Applied Thermal Engineering, 25* (2005), pp. 2966-2982.

[31] Amelio, M., Morrone, P., Numerical evaluation of the Energetic Performances of Structured and Random Packed Beds in regenerative thermal oxidizers, *Applied Thermal Engineering, 27* (2007), pp. 762-770.

[32] Amelio, M., Florio, G., Morrone, P., Senatore, S., The influence of rotary valve distribution systems on the energetic efficiency of regenerative thermal oxidizers (RTO), *International Journal of Energy Research, 32* (2008), pp. 24-34.

[33] Duffie, J. A., Beckman, W. A., Solar Engineering of Thermal Processes, Wiley-Interscience publication, Winsconsin, 1991.

[34] Gupta, A. S., Thodos, G., Direct analogy between mass and heat transfer to beds of spheres, *A.I.Ch.E. Journal, 9* (1973), 6, 751-754.

[35] Lof, G. O. G., Hawley, R. W., Unsteady State Heat Transfer Between Air and Loose Solids, *Industrial and Engineering Chemistry, 40* (1948), 6, pp. 1061-1070.

[36] Kunii, D., Levenspiel, O., Fluidization Engineering, Second Edition, Butterworth-Heinemann, Newton, 1991.

[37] Achenbach, E., Heat and Flow Characteristics of Packed Beds, *Experimental Thermal and Fluid Science, 10* (1995), pp. 17-27.

[38] Morrone, P., Di Renzo, A., Di Maio, F. P., Amelio, M., Modelling process characteristics and performance of fixed and fluidized bed Regenerative Thermal Oxidizer (RTO), *Industrial & Engineering Chemistry Research, 45* (2006), pp. 4782-4790.

[39] Algieri, A., Amelio, M., Morrone, P., A numerical analysis of energetic performances of active and passive aftertreatment systems, *International Journal of Energy Research, 33* (2009), 7, pp. 696-708.

[40] Algieri, A., Amelio, M., Bova, S., Morrone, P., Active and Passive Aftertreatment Systems: A Numerical Analysis of Energetic Performances, *Proceedings*, ICAT '08 Conference, Istanbul, Turkey, 2008.

[41] Algieri, A., Amelio, M., Morrone, P., Energetic Analysis of the Performances of Innovative Aftertreatment Systems, *Proceedings*, SAE 2009 Powertrains, Fuels and Lubricants Meeting, Florence, Italy, SAE paper 2009-01-1948, 2009.

[42] Algieri, A., Morrone, P., The influence of the operating conditions on the performances of innovative aftertreatment systems, *Proceedings*, 12th European Automotive Congress - EAEC 2009, Bratislava, Slovakia, 2009.